FINAL REPORT **NKFI-identifier:** 101591
Title of the project: Comparative studies on homodimeric aspartyl proteases

Detailed scientific report of the research

Characterization of retroviral, retrotransposon and cellular homodimeric aspartic proteases

HTLV-2 and HTLV-3 proteases

Coding sequences of human T-lymphotropic virus type 2 and 3 (HTLV-2 and HTLV-3) proteases (codon optimized for bacterial expression) were cloned into pET11 expression plasmids and transformed into BL21(DE3) *E.coli* cells. The MBP-fused forms of full-length HTLV-2 and HTLV-3 protease sequences were also cloned. Optimization of protein expression was followed by purification of the recombinant proteins.

Enzyme specificities were studied using synthetic oligopeptide substrates representing the naturally occurring cleavage sites of HTLV-1, HTLV-2, and HTLV-3 proteases. All the studied oligopeptides were found to be effective substrates for HTLV-2 and HTLV-3 proteases suggesting higher similarities in the specificity of these enzymes as compared to that found comparing HIV-1 and HIV-2 proteases.

Amino acid preferences of HTLV-2 and HTLV-3 proteases have also been studied to be able to compare them to those of HTLV-1 PR (**Figure 1**). Oligopeptide substrates representing the wild type and modified versions of HTLV-1 capsid/nucleocapsid (CA/NC) cleavage site (KTKVL*VVQPK) were chosen for the *in vitro* specificity studies. Both shortened and P4, P3, P2, P1, and P1' substituted sets of substrates were used that were previously utilized to characterize the specificity of HTLV-1 protease (Sperka et al., 2007).

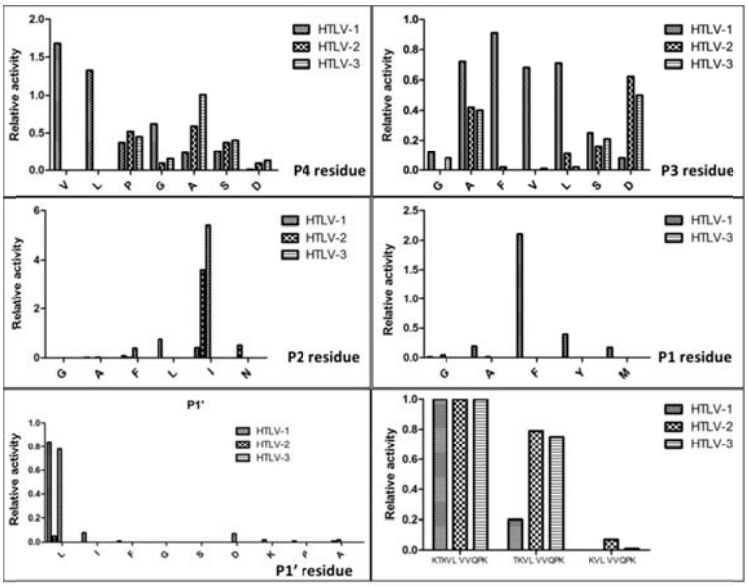

Figure 1. Comparison of the relative activities (%) obtained for selected P4, P3, P2, P1, and P1'-substituted or truncated variants of KTKVL*VVQPK substrates for HTLV-1, HTLV-2 and HTLV-3 PRs. Relative activities were expressed relative to that obtained with the KTKVL*VVQPK substrate. Values for HTLV-1 PR have been published previously (Sperka et al., 2007).

Shortened versions of the wild type HTLV-1 CA/NC cleavage site substrates (TKVL*VVQPK and KVL*VVQPK) were also used to study the size of substrate binding site (**Figure 1**). The unmodified decapeptide was the best, while the shortest form was the least effective substrate for both HTLV-2 and HTLV-3 proteases. This result suggests that these proteases have extended substrate-binding sites, in good agreement with the values measured for HTLV-1 protease (Sperka et al., 2007). HTLV-1 PR was found to have a more extended substrate binding region as compared to those of bovine leukemia virus (BLV) and HIV-1 proteases, as those

enzymes cleaved the shortened substrates more efficiently compared to the decapeptide form (Sperka et al., 2007).

Comparative analysis of the structural determinants for amino acid preferences and evaluation of *in vitro* specificity studies are still in progress in the case of HTLV PRs. Our results measured on HTLV-2 and HTLV-3 proteases are comparable with the previously published values of HTLV-1, BLV and HIV-1 proteases, because the same substrate set was used in our analyses (Sperka et al., 2007).

PEG10 protein

The paternally expressed gene 10 (PEG10) human cDNA sequence was modified by insertional mutagenesis to produce a frameshift-mutant RF1/RF2 encoding sequence; a single adenine was inserted into the "slippery" heptanucleotide sequence to provide the transcription of the whole RF1/RF2 encoding mRNA. The coding sequence (followed by a thrombin cleavage site) was successfully cloned into a pQE-TriSystem-HisTrap plasmid. A S26A mutant containing mutation in the active center of protease was also generated for PEG10 protein, which was expected to fully inactivate the protease based on the previously published studies on HIV-1 protease (Strisovsky et al., 2000). In our studies the frameshift mutant PEG10 RF1/RF2 protein was considered as the wild type protein.

Proteolytic processing of the PEG10 RF1/RF2 fusion protein expressed in bacterial expression system was observed, but the S26A fireman's-grip mutant also showed similar processing, which indicated that this cleavage was not catalyzed by the PEG10 protease. Therefore, we switched to eukaryotic protein expression.

Western blot analyses (using antibodies developed against the fusion tag or PEG10 protein) showed a higher molecular weight for the PEG10 RF1/RF2 protein overexpressed in 293T human cells than it was expected based on software calculations (73 kDa) (**Figure 3**). This difference is thought to be due to a possible posttranslational modification that needs to be explored by mass spectrometry.

The PEG10 RF1/RF2 protein was found to be processed due to its autoproteolytic activity (**Figure 3**), in good agreement with its previously described activity (Clark et al., 2007). Time course analysis of PEG10 autoprocessing also confirmed the proteolytic activity of the protease. pH 7.0 buffer was used in our experiments, because no proteolytic activity was detected in pH 5.0 buffer. While S26A mutant showed no self-processing activity in the inhibition studies (**Figure 3**), results of other experiments were ambiguous and did not proved the full inactivation of the this mutant. To clarify whether the fireman's-grip mutation impairs the protease activity, we have already started mutagenesis to produce a protein bearing mutation of the catalytic aspartate (D25A) of the protease domain. The fully inactivated protein will be used as negative control in protease activity assays, furthermore, studying the anti-apoptotic and proliferative effects of PEG10 is also in progress with the wild-type and active site mutant proteins.

MSRV protease

We have analyzed the primary structure of the multiple sclerosis associated retrovirus (MSRV) protease and predicted both its secondary and tertiary structural organization. Based on the analysis of amino acid sequence we predicted, that the MSRV may encode a functional protease, because its predicted fold is consistent with those of other retroviral PRs; it contains the conserved -DT/SGA- active site sequence motif and a second conserved motif (-GRD-) near the C-terminal end, the spacing between the two conserved sequence motifs is consistent with that of other retroviral PRs, there are no long insertions or deletions in the sequence, and the putative C-terminal β-sheets are predicted to be capable of dimer interface formation.

To characterize the MSRV PR experimentally, the synthetic gene of MSRV PR (containing potential proteolytic processing sites) cloned into an expression vector was transformed into *E. coli* cells, followed by expression of GST-fused protein and its purification by affinity chromatography.

No proteolytic activity was detected for MSRV in autoproteolysis studies or activity measurements using oligopeptide substrates.

ASPRV1 protein

We have prepared the expression clone of the 28 kDa precursor form of skin-specific retroviral-like aspartic protease ASPRV1. Autoprocessing studies and protease assays using oligopeptide substrates were performed to prove that the active form of the protein can be expressed in *E. coli* cells. Autoprocessing sites of the protein were mutated (A189K/N190I and A167G/L168G/A189K/N190I mutants were generated) to compare the activities of the precursor (p28) and processed (p14) forms. While the double mutant having mutations at the main autoproteolytic cleavage site was found to retain its self-processing activity, the quadruple mutant having mutations at both self-processing sites showed no self-processing and only negligible activity on exogenous substrates, indicating that the precursor form's proteolytic activity is substantially lower compared to that of the fully processed form, similarly as it was found for retroviral (like HIV-1) proteases.

Activity of ASPRV1 PR was found to be boosted by high ionic strength, similarly to the retroviral proteases. However, the pH optimum of the enzyme was weakly acidic pH (6.78 ± 0.85), similarly to that of the mouse orthologue of the enzyme; this is higher that the pH optimum of retroviral proteases, and is close to the physiological pH of *stratum granulosum* and ASPRV1 PR could therefore be active at the weakly acidic pH of *stratum corneum*.

Dimer stability of ASPRV1 PR was also studied. The dimer dissociation constant (K_d) was found to be much higher, while the urea dissociation constant (UC_{50}) of ASPRV1 was lower than that of HIV-1 PR. The differences in the dimer stabilities were explained based on results of structural analyses. While alternating, intertwined N- and C-terminal β-sheets in the dimer interface of HIV-1 PR provides stronger interaction between the monomers, there is no such interactions in the dimer interface of ASPRV1 PR (consisting of only C-terminal β-sheets) which causes lower stability of the homodimer. Both dimer interface organization and dimer stability (urea dissociation constant) of ASPRV1 closely resembles to those of XMRV PR (**Matúz et al., 2012**).

Catalytic efficiency of wild type and mutant ASPRV1 enzymes was measured on different oligopeptide substrates representing the wild type and modified versions of the natural cleavage sites of ASPRV1 and HIV-1 proteases. A wild type and a P4-phosphorylated version of GSFLY*QVSTH substrate representing the cleavage site present in the linker sequence connecting the subdomains of filaggrin molecule were also used for activity measurements. While the wild type substrate was cleaved, the P4-Ser phosphorylated variant was not a substrate for ASPRV1. This is in good agreement with the proposed role of cleavage site phosphorylation, which prevents premature processing of filaggrin and contributes to the regulation of the proteolysis.

The aim of our cell culture experiments was to study the role of ASPRV1 in the differentiation of HaCaT cells. HaCaT cell differentiation was induced by using Ca^{2+}-supplemented (2 mM) cell culture medium, and substantial morphological changes have were observed compared to the non-differentiated cells cultured in medium containing Ca^{2+} only in low concentration. Preliminary wound healing experiments showed faster regeneration for cells cultured in Ca^{2+}-supplemented medium. To follow expression of ASPRV1 and filaggrin, both Western blot (anti-ASPRV1, anti-filaggrin antibodies) and qPCR experiments have been performed. Overexpression of the 28 kDa form of ASPRV1 was achieved successfully by using retroviral gene transfer utilizing the HIV-1 based vector system, but the cells were unable to overexpress the mature, 14 kDa ASPRV1 PR.

Ty1 protease

pET11 bacterial expression plasmids bearing the coding sequence of Ty1 PR or Ty1 Gag-PR-His_6 proteins were transformed into *E.coli* cells. Ty1 Gag-PR- His6 recombinant protein was

found to be processed during its purification by affinity chromatography, resulting Ty1 PR-His_6 protein. Both the precursor and the processed forms were detected by Western blot. This proteolytic event suggested the self-processing of Ty1 protease. The processed Ty1 PR-His_6 fusion protein was used for the proteolytic assays using different synthetic oligopeptide substrates representing the wild type of modified cleavage sites of Ty1, Ty3, or HIV-1 proteases. VPTIN*NVHTS substrate representing the Ty1 PR/IN cleavage site was found to be an efficient substrate for the enzyme. Enzyme kinetic measurements were also performed to determine kinetic parameters for Ty1 protease, furthermore, pH optimum of the enzyme was also measured and was found to be close to 30°C. We have also attempted to express active Ty3 protease using various expression systems and also yeast cells but so far these attempts were not successful.

TEV and Rhinovirus 3C proteases as tools for protein expression

We have reviewed the application of proteolytic enzymes in life sciences with an emphasis on their molecular biological applications (**Mótyán et al., 2013b**). Tobacco etch virus (TEV) and human rhinovirus 3C (R3C) proteases having important role in fusion-tag removal were also included in this review, and have been studied previously by us in collaboration with Dr. David Waugh (Kapust et al., 2002). The high specificity of these viral proteases ensures the precise removal of the target proteins, with low frequency of unwanted protein cleavages. We have been involved in the studies of these enzymes with the interest of achieving better expression systems for our own studies. In a comparative study, R3C protease was found to be 10-fold more active at 4°C (temperature generally used for fusion tag removal) compared to TEV protease (**Raran-Kurussi S et al., 2013**).

Inhibition studies

Inhibition profiling of aspartic protease inhibitors can facilitate the identification and/or design of molecules which have broad specificity on retroviral and retroviral-like proteases, or might aid the identification of molecules which are specific for cellular homodimeric aspartyl proteases and might be suitable for cell culture studies.

Inhibition studies were performed for each HTLV proteases to study the inhibitory potential of IB268 (KTKVL-r-VVQPK) and IB269 (APQVL-r-PVMHP) molecules, which are reduced peptide (“r”) analogues of HTLV-1 cleavage sites. Lowest K*i* values were determined for HTLV-1 PR, but both molecules inhibited HTLV-2 and HTLV-3 proteases efficiently. IB268 was found to be more effective inhibitor for all HTLV proteases (**Figure 2**), in good agreement with the previous inhibition studies on HTLV-1 PR (Sperka et al., 2007).

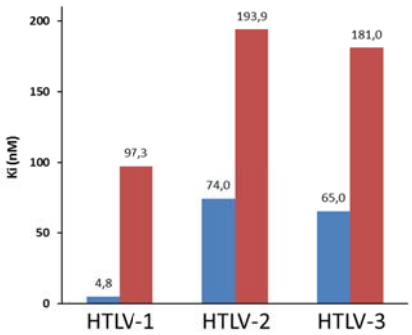

Figure 2. Inhibitory effect IB268 (blue columns) and IB269 (red columns) inhibitors on HTLV proteases.

Inhibitory effect of indinavir and pepstatin A molecules were tested on autoprocessing of overexpressed PEG10 protein. Both molecules were found to impair autoproteolytic activity of wild type PEG10, while no self-processing of the active site mutant was observed (**Figure 3**).

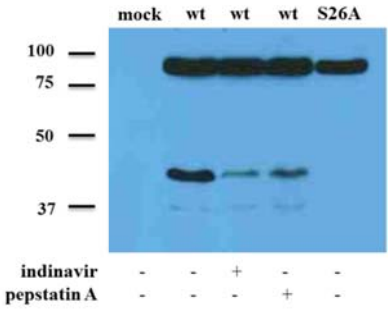

Figure 3. Inhibitory effect of indinavir and pepstatin A on PEG10 autoprocessing in buffer pH 7.0. Western blot analysis was performed using anti-PEG10 antibody. Abbreviation: wt - wild-type PEG10 PR; S26A - active site mutant PEG10 PR.

The kinetic properties of pepstatin A and acetyl-pepstatin inhibitors were studied for XMRV and HIV-1 PRs by using pepstatin A and acetyl-pepstatin molecules. Dimerization and urea dissociation constants have also been determined for both proteases (**Matúz et al., 2012**). To study the possible binding modes of pepstatin A and acetyl-pepstatin molecules to HIV-1 and XMRV proteases, interaction energies were calculated for the different inhibitor binding modes. Calculations suggested strong preference for the one-inhibitor binding mode for HIV-1 PR-acetylpepstatin and the two-inhibitor binding mode for XMRV PR-pepstatin A interactions. Crystallographic studies revealed mixed type of binding of acetyl-pepstatin to XMRV PR, while binding of two inhibitor molecules (as substrate analogs) were observed for XMRV PR, binding of only one inhibitor molecule (as a transition state analog) was seen in the case of HIV-1 PR. Inhibition constants determined for XMRV and HIV-1 PRs also indicated more effective inhibitory effect for the binding of a acetyl-pepstatin single inhibitor molecule. The docking and interaction energy calculation methods applied for the characterization of enzyme-inhibitor complexes of XMRV PR were in good agreement with the data obtained from the crystallographic studies (Li et al., 2011) (**Matúz et al., 2012**).

To study the inhibitory effects of HIV-1 PR inhibitors on purified ASPRV1 protease, we have tested seven inhibitors commonly used in antiretroviral therapies (indinavir, amprenavir, tipranavir, saquinavir, ritonavir, darunavir, and nelfinavir) using an oligopeptide substrate. Only indinavir was found to be effective inhibitor of ASPRV1 PR, in good agreement with the findings on the self-processing capability (Bernard et al., 2005). The inhibition constant for indinavir was also determined (Ki = 0.94 μM ± 0.12) and was found to be much higher than in the case of HIV-1 and HIV-2 proteases (Brower et al., 2008), but significantly lower than inhibitory constant in the case of BLV (Sperka et al., 2007) or HTLV-1 proteases (Bagossi et al., 2004). The inhibition of ASPRV1 by indinavir could explain the inhibitor's side effects on the skin in the case of AIDS therapy (Bernard et al., 2005).

To complement our previous and recent inhibitor profiling studies, inhibitory potentials of molecules commonly used in antiretroviral therapies were tested for HIV-1 and HIV-2 proteases, as well. The susceptibility of HIV-1 and HIV-2 PR was measured against amprenavir, which was found to be less effective inhibitor of HIV-2 protease compared to HIV-1 PR (**Tie et al., 2012**). A more detailed inhibition study was also performed for HIV-2 protease, to explore the efficacy of clinically used protease inhibitors in the case of the wild type and a treatment-associated resistance mutation-containing (I54M/L90M double mutant) HIV-2 proteases. A wild type HIV-2 vector backbone and cloning techniques were used to develop a cassette system for inhibitor profiling (**Mahdi et al., 2014**). Using this modular HIV-2 protease cassette system, enzymatic and cell culture inhibition assays were performed. We found that darunavir, indinavir, saquinavir, and lopinavir were the most potent inhibitors of HIV-2 protease, furthermore, double resistance-mutations led to decrease in the inhibitory effect of the inhibitors, with the exception of tipranavir (**Mahdi et al., 2015**). Not only a double-mutant HIV-2 protease, but an extreme drug-resistant multiple mutant HIV-1 protease was also studied (**Louis et al., 2013**). Our main goal in general was

to compare the specificity and dimer stability of homodimeric aspartic proteases. As several residues are introduced by drug resistance mutations into the substrate binding site that are found in the equivalent position of other retroviral PRs, inhibition studies on retroviral or retroviral-like cellular aspartic proteases can help to understand the fundamental characteristics of these enzymes.

In silico approaches used for structural analyses

Secondary structures were predicted for the studied homodimeric aspartic proteases. Tertiary structures were also predicted by homology modeling for the proteases of which crystal structure have not been solved till now (Ty1, MSRV, ASPRV1, PEG10). The proposed model structures were further analyzed to identify residues of substrate binding sites or used for energy minimization or binding calculations. Crystal structures of human and yeast Ddi1, and EAIV proteases were used as template structures for homology modeling of cellular retroviral-like proteases (PEG10, ASPRV1). To complement our dataset of cellular retroviral-like proteases, we also performed homology modeling and structural analyses on Ddi1 proteases. Flap regions of Ddi1 proteases which are disordered in the electron density maps were built up based on structure of EIAV PR.

Comparative structural analyses revealed that Ty1, ASPRV1, and PEG10 proteases share the fold of retroviral PRs and contain an additional helical insert which was not described previously for these enzymes (**Figure 4**). This helical region is not found in most retroviral PRs but is present in EIAV retroviral (1FMB.pdb) and in Ddi1 retroviral-like proteases (2I1A.pdb and 3S8I.pdb), as it was revealed based on crystallographic studies. Secondary and tertiary structure predictions suggested a six-stranded dimer interface organization for ASPRV1 and PEG10 PRs which consists of only C-terminal β-sheets and closely resembles to that of Ddi1 PR and similar to that of XMRV PR (**Figure 4**). Dimer interface of Ty1 PR was also predicted to show no alternating strands and consists of only C-terminal β-sheets. Our results indicate structural similarities between these homodimeric cellular aspartic proteases and other retroviral (XMRV) and retroviral-like (Ddi1) proteases. Fold of XMRV and Ddi1 PRs have been found to be similar to those of other retropepsins (like HIV-1), although with some characteristic differences; particularly their dimer interface appears to be similar to those of the monomeric, pepsin-like enzymes. On the other hand, the architecture of the active site of XMRV and Ddi1 PRs is rather similar to that of other retropepsins, therefore detailed studies are required to identify conserved structural features.

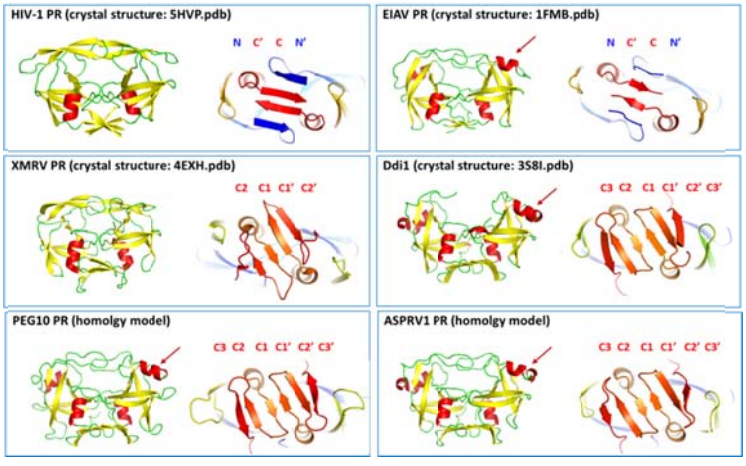

Figure 4. Tertiary structures of some retroviral and retroviral-like cellular PRs. Front views of the proteases are indicated (left parts), red arrows show additional helical inserts. Dimerization regions are enlarged (right parts), the N-terminal regions of molecules are blue, the C-terminal regions are red. Dimer interface organization is also indicated by blue and red letters.

Previously we have studied the substrate specificity of eleven retroviral PRs representing all retroviral *genera* (Bagossi et al., 2005; Eizert et al., 2008). That method was successfully adapted for Ddi1, PEG10, and ASPRV1 proteases to calculate the substrate binding site cavities (**Figure 5**). This calculation algorithm has already been developed and applied for HTLV-1 PR (Bagossi et al., 2005; Eizert et al., 2008) and is being used in the case of HTLV-2 and HTLV-3 PRs. Characterization of the similarities and differences between the enzyme specificities can facilitate the inhibitor design and might correspond to the identification of broad-spectrum protease inhibitors.

Structural models of enzyme-substrate complexes were successfully used to study the specificity-determining features of ASPRV1 protease and interpret the results of *in vitro* specificity studies. Nine P3-substituted VSQNY*PIVQ oligopeptides representing modified HIV-1 matrix/capsid (MA/CA) cleavage sites were tested in protease assay and only the P3-Lys modified version was found to be efficient substrate for the enzyme (**Figure 5**), in good agreement with the predicted favorable interactions between the P3-Lys residue of VSKNY*PIVQ substrate and the Tyr7 residue of ASPRV1 S3 binding site.

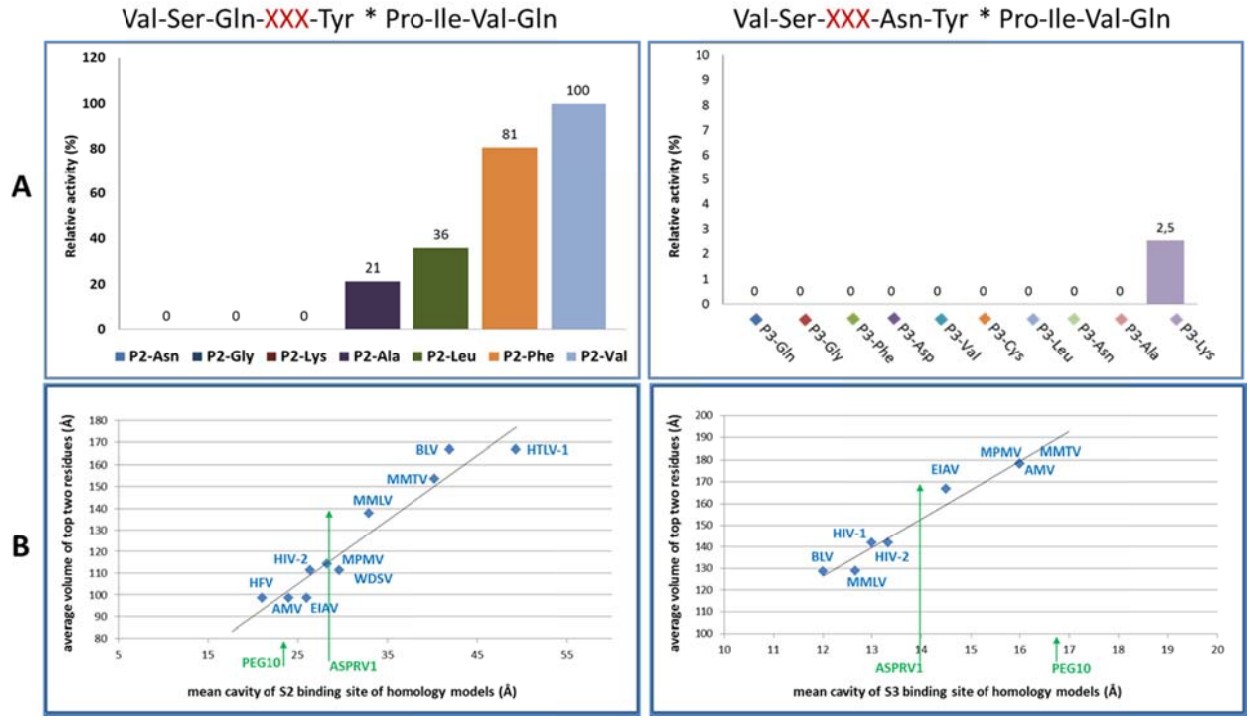

Figure 5. A) Comparison of relative activities of ASPRV1 PR on peptides representing the wild type (VSQNY*PIVQ) and P2 or P3 modified HIV-1 MA/CA cleavage sites. Relative activities were expressed as activity relative to that obtained with the VSQVY*PIVQ substrate. **B)** Mean cavity volumes of S2-S3 subsites of various PRs versus the average volume of the two residues for which the measured relative activity was the highest (Bagossi et al., 2005; Eizert et al., 2008) (blue). Mean cavity volumes were calculated for ASPRV1 and PEG10 PRs, as well (green). Average volume of Val/Phe (P2) and volume of Lys (P3) residues were used to plot data for ASPRV1 PR.

Two dimer interface mutants have also been designed for ASPRV1 PR using the proposed model structures to study the contribution of the interface strands to dimer stability. While the Δ(K118-E136) mutant lacks C3 and C3' outer interface strands, the residues responsible for inner C1-C1' β-sheet interactions were modified in the case of N103G/D107G/E109G/K116G mutant. While truncation of the predicted outer β-sheets dramatically decreased the catalytic efficiency (**Figure 6**), the mutations preventing the predicted inner β-sheet interactions completely eliminated the activity. Results of *in vitro* activity measurements are in good agreement with the predicted effects of mutations, indicating that outer strands of the six-stranded interface contribute to dimer

stability, while modified residues of inner strands are involved in the hydrogen bond network formation of dimer interface and are necessary for inter- and intramonomeric interactions.

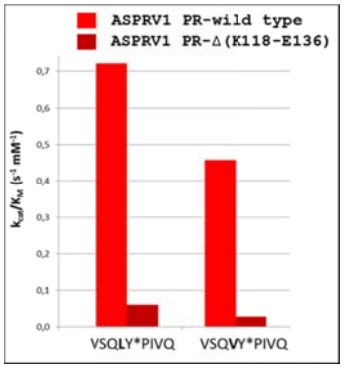

Figure 6. Catalytic efficiencies of wild type and dimer interface mutant ASPRV1 PRs were measured with oligopeptide substrates representing P2L and P2V mutants of wild type HIV-1 MA/CA cleavage site.

Instead of the originally proposed study on the effect of dimerization interface type on the protease stability by the characterization of XMRV/HIV chimera enzymes, comparative study of XMRV, ASPRV1 and HIV-1 proteases have been performed. The mode of dimerization of HIV-1 and XMRV proteases have been analyzed by comparing crystal structures and dimerization constants determined by enzyme kinetic experiments (**Matúz et al., 2012)**. Wild type ASPRV1 protease having a six-stranded dimer interface was modified by the truncation of outer interface strands, resulting in a mutant enzyme having a four-stranded, XMRV-like interface. Similar dimer dissociation constant values were determined for these enzymes, which were found to be significantly lower compared to HIV-1 PR, which also has a four-stranded interface, but the alternating nature of strands provides higher dimer stability for HIV-1 PR.

As homology modeling approaches have been successfully used to examine structural characteristics of retroviral and cellular retroviral-like proteases, it gave the opportunity to study the NOD-like receptor family CARD domain containing 5 (NLRC5) protein (Neerincx et al., 2010), as well, of which importance has been implicated in viral infections as being part of the innate immune system. Sequence alignments were used to identify consensus patterns of leucine-rich repeat sequences and homology models were prepared for both the monomeric and homo-heptameric forms of the full-length human protein (**Mótyán et al., 2013a**). We have performed experiments with the aim of the biochemical characterization of NLRC5 protein (**Mótyán et al., 2016, submitted for publication**) to correlate the biochemical findings with the homology models (**Mótyán et al., 2013a**). A selected reaction monitoring-based targeted proteomic approach was also developed, validated, and applied for the detection and quantitative measurement of human NLRC5 protein. This antibody-free method was used to measure the changes in endogenous NLRC5 protein levels in treated and untreated HaCaT cells (**Mótyán et al., 2016, submitted for publication**).

Effects of mutations on the protein structure need to be considered in mutation design, therefore, besides the secondary and tertiary structure prediction methods applied in our studies, other approaches were also tested for predicting changes in the protein stability upon point mutations. Data in the literature suggested that among all HIV-1 proteins, the capsid protein (CA) has the highest rigidity and least tolerance toward mutations. Stability changes of HIV-1 CA caused by the mutations of previously identified cleavage sites were predicted. Predicted effects were found to be in good agreement with the results of circular dichroism spectroscopy measurements and cyclophilin A binding assays (**Tóth et al., 2016, submitted for publication**), indicating the reliability of the applied prediction algorithm.

References

(Published and submitted articles supported by this OTKA grant are cited in bold)

Bagossi P, Kádas J, Miklóssy G, Boross P, Weber IT, Tözsér J. Development of a microtiter plate fluorescent assay for inhibition studies on the HTLV-1 and HIV-1 proteinases. *J Virol Methods.* 2004; 119: 87-93.

Bagossi P, Sperka T, Fehér A, Kádas J, Zahuczky G, Miklóssy G, Boross P, Tözsér J. Amino acid preferences for a critical substrate binding subsite of retroviral proteases in type 1 cleavage sites. *J Virol.* 2005; 79: 4213-8.

Bernard D, Méhul B, Thomas-Collignon A, Delattre C, Donovan M, Schmidt R. Identification and characterization of a novel retroviral-like aspartic protease specifically expressed in human epidermis. *J Invest Dermatol.* 2005; 125: 278-287.

Brower ET, Bacha UM, Kawasaki Y, Freire E. Inhibition of HIV-2 protease by HIV-1 protease inhibitors in clinical use. *Chem Biol Drug Des.* 2008; 71: 298-305.

Clark MB, Janicke M, Gottesbuhren U, Kleffmann T, Legge M, Poole ES, Tate WP. Mammalian gene PEG10 expresses two readingframes by highefficiency -1 frameshifting in embryonic-associated tissues. *J BiolChem.* 2007; 282: 37359-69.

Eizert H, Bander P, Bagossi P, Sperka T, Miklóssy G, Boross P, Weber IT, Tözsér J. Amino acid preferences of retroviral proteases for amino-terminal positions in a type 1 cleavage site. *J Virol.* 2008; 82: 10111-7.

Kapust RB, Tözsér J, Copeland TD, Waugh DS. The P1' specificity of tobacco etch virus protease. *Biochem Biophys Res Commun.* 2002; 294: 949-55.

Li M, Gustchina A, Matúz K, Tözsér J, Namwong S, Goldfarb NE, Dunn BM, Wlodawer A. Structural and biochemical characterization of the inhibitor complexes of xenotropic murine leukemia virus-related virus protease. *FEBS J.* 2011; 278: 4413-24.

Louis JM, Tözsér J, Roche J, Matúz K, Aniana A, Sayer JM. Enhanced stability of monomer fold correlates with extreme drug resistance of HIV-1 protease. *Biochemistry.* 2013; 52: 7678-88.

Mahdi M, Matúz K, Tóth F, Tőzsér J. A modular system to evaluate the efficacy of protease inhibitors against HIV-2. *PLOS ONE.* 2014, 9:(11) p. e113221.

Mahdi M, Szojka Z, Mótyán JA, Tőzsér J. Inhibition Profiling of Retroviral Protease Inhibitors Using an HIV-2 Modular System. *Viruses.* 2015; 7: 6152-62.

Matúz K, Mótyán J, Li M, Wlodawer A, Tőzsér J Inhibition of XMRV and HIV-1 proteases by pepstatin A and acetyl-pepstatin. *FEBS J.* 2012; 279: 3276-86.

Mótyán JA, Bagossi P, Benkő S, Tözsér J. A molecular model of the full length human NOD-like receptor family CARD domain containing 5 (NLRC5). *BMC Bioinformatics.* 2013a; 14: 275.

Mótyán JA, Tóth F, Tőzsér J. Research Applications of Proteolytic Enzymes in Molecular Biology. *Biomolecules.* 2013b; 3: 923-942.

Mótyán JA, Farkas B, Kalló G, Csősz É, Benkő Sz, Tőzsér J. Development of an antibody-free selected reaction monitoring-based method for quantification of human NOD-like receptor family CARD domain containing 5 (NLRC5) protein. *Manuscript submitted for publication.*

Neerincx A, Lautz K, Menning M, Kremmer E, Zigrino P, Hösel M, Büning H, Schwarzenbacher R, Kufer TA. A role for the human nucleotide-binding domain, leucine-rich repeat-containing family member NLRC5 in antiviral responses. *J Biol Chem.*2010; 285: 26223-32.

Raran-Kurussi S, Tözsér J, Cherry S, Tropea JE, Waugh DS. Differential Temperature Dependence of Tobacco Etch Virus and Rhinovirus 3C Proteases. *Anal Biochem* 2013, 36(2): 142-4.

Sperka T, Miklóssy G, Tie Y, Bagossi P, Zahuczky G, Boross P, Matúz K, Harrison RW, Weber IT, Tözsér J. Bovine leukemia virus protease: comparison with human T-lymphotropic virus and human immunodeficiency virus proteases. *J Gen Virol.* 2007; 88: 2052-63.

Strisovsky K, Tessmer U, Langner J, Konvalinka J, Kräusslich HG. Systematic mutational analysis of the active-site threonine of HIV-1 proteinase: rethinking the "fireman's grip" hypothesis. *Protein Sci*. 2000; 9: 1631-41.

Tie Y, Wang YF, Boross PI, Chiu TY, Ghosh AK, Tözsér J, Louis JM, Harrison RW, Weber IT. Critical differences in HIV-1 and HIV-2 protease specificity for clinical inhibitors. *Protein Sci.* 2012; 21: 339-50.

Tóth F, Kádas J, Mótyán JA, Tőzsér J. Effect of internal cleavage site mutations in human immunodeficiency virus type 1 capsid protein on its structure and function. *Manuscript submitted for publication.*